Bangladesh J. Plant Taxon. **31**(2): 239-264, 2024 (December) DOI: https://doi.org/10.3329/bjpt.v31i2.78751

INTEGRATING TAXONOMY AND DRUG DISCOVERY: LILIOPSIDA FLORA OF RAJBARI, BANGLADESH TARGETING *AMORPHOPHALLUS PAEONIIFOLIUS* FOR COLORECTAL CANCER THERAPY

MIRUNA BANU, SHEIKH SUNZID AHMED, MOMTAZ BEGUM AND M. OLIUR RAHMAN*

Department of Botany, University of Dhaka, Dhaka 1000, Bangladesh

Keywords: Liliopsida; *Amorphophallus paeoniifolius*; MMP-9; Molecular docking; Dynamics simulation; MM/GBSA; Bioinformatics.

Abstract

The present study explores the angiosperm flora belonging to the class Liliopsida in Rajbari district, seamlessly integrating taxonomy with phytocompound-based drug discovery through advanced computational biology approaches. The study covered all five upazilas (sub-districts) of the district. A total of 201 taxa across 118 genera and 24 families of Liliopsida were identified. The flora is predominantly composed of herbs (79.06%), followed by climbers (7.96%), trees (7.46%), shrubs (2.98%), and a minimal occurrence of epiphytes (1.99%). Poaceae emerged as the largest family, comprising 58 taxa across 36 genera, followed by Araceae (26 taxa) and Cyperaceae (17 taxa). Notably, the study identified 25 medicinal plant species under Liliopsida. Some rare species within Liliopsida, such as *Coix aquatica, Wolffia arrhiza, Typha domingensis,* and *Schumannianthus benthamianus* were also recorded in the study area. Among the medicinal plants identified, *Amorphophallus paeoniifolius* (Dennst.) Nicolson was selected for further investigation into colorectal cancer drug discovery. The computational therapeutics design endeavor unveiled two lead compounds: Riboflavin (-7.9 kcal/mol) and Lupeol (-6.1 kcal/mol), both of which demonstrated promising favorable drug-likeness properties. Molecular dynamics simulation spanning 100 ns revealed structural stability of the identified leads. PCA and Gibbs free energy landscape study further corroborated the drug-candidacy of the leads. DFT-based molecular reactivity study unveiled Lupeol as the most kinetically stable compound (6.915 eV). The findings highlight the significance of multi-disciplinary approach integrating classical taxonomy with bioinformatics and pave the way for future colorectal cancer therapeutics.

Introduction

The Convention on Biological Diversity (CBD) has underscored the pivotal role of taxonomic and vegetation studies in ensuring effective biodiversity conservation. Such studies provide fundamental data on species identification, distribution, and classification, which are crucial for crafting well-informed conservation strategies. The CBD highlights that a lack of comprehensive taxonomic knowledge, coupled with a shortage of trained taxonomists and inadequate infrastructure, creates a significant "taxonomic impediment" that hampers efforts to assess and safeguard global biodiversity. Addressing this impediment is vital for achieving the CBD's objectives, as it facilitates precise documentation of species diversity, helps identification of conservation priorities, and allows for effective monitoring of ecosystem changes over time. The CBD thus advocates for enhanced investment in taxonomic research and capacity building to support sustainable biodiversity management and policy development (Heywood, 2004).

Rajbari district is geographically positioned between 22°40` and 23°50` N latitudes and between 89°19` and 90°40` E longitudes, covering an area of 1,119 sq. km. The district enjoys a

*Corresponding author: oliur.bot@du.ac.bd

moderate tropical monsoon climate characterized by three distinct seasons: a hot summer, a rainy season, and a dry winter. The annual average temperature ranges from a minimum of 9.8°C to a maximum of 30.1°C. Relative humidity remains fairly consistent throughout year, fluctuating from 77 to 79%. The annual rainfall is approximately 3742 mm (BBS, 2022). Rajbari district comprises 5 upazilas, namely Rajbari Sadar, Pangsha, Baliakandi, Kalukhali and Goalanda with an area of 347.1, 313, 242.53, 157.14 and 149 sq. km, respectively. Rajbari district encompasses a variety of habitats, including wetlands, cultivated land, charland, fallow land, scrub jungles and homestead areas. As an agriculturally rich region, its plant genetic, species and ecosystem diversity significantly influence the local environment. However, the floristic compositions are declining due to increasing urbanization, industrialization, habitat fragmentation, road construction, agricultural expansion, mismanaged brickfields as well as other human activities. Given the ongoing trend of habitat degradation and fragmentation, many species could disappear from the region before they are even documented and studied.

Building upon the foundational works of Hooker (1872–1897) and Prain (1903), numerous floristic endeavors have been conducted within the present political boundaries of Bangladesh, including different upazilas and protected areas (Rahman *et al*., 2012, 2013, 2019a,b; Rahman and Alam, 2013; Sarker *et al*., 2013; Rahman and Hassan, 1995; Islam *et al*., 2009; Uddin and Hassan 2010, Arefin *et al*., 2011; Rahman *et al*., 2015; Haque *et al*., 2018). Despite these efforts, only a few district-level floras have been produced, such as those for Gazipur (Tabassum 2015), Patuakhali (Sultana, 2012), Bagerhat (Hossain *et al*., 2022), Satkhira (Hossain *et al*., 2021) and Narsingdhi (Khanam and Khan, 2020; Khanam *et al*., 2020). However, the floral diversity of Rajbari district has yet to be explored through detailed field inventories and specimen examination, leaving much of its flora unexplored.

Plant taxonomy and floristics are essential for the precise detection of medicinal taxa, forming the foundation for exploring their therapeutic potential. By systematically classifying plants and understanding their distribution, taxonomists can identify species traditionally used in medicine or those possessing bioactive compounds, thus providing a gateway to drug discovery. This taxonomic accuracy is critical in ensuring the correct selection of plants for phytochemical analysis, driving the development of novel drugs through natural compounds. Compared to synthetic drugs, natural products offer several advantages, such as greater structural diversity, better biocompatibility, lower toxicity, and improved efficacy in targeting biological systems. These compounds, refined by evolution over thousands of years, are inherently optimized for biological interactions, making them a valuable resource in modern drug discovery (Ahmed and Rahman, 2024; Ahmed *et al*., 2024).

Structure-based drug design (SBDD) integrates this taxonomic knowledge by leveraging advanced computational techniques to accelerate the drug discovery process. SBDD focuses on analyzing the three-dimensional structure of target proteins and identifying compounds, such as phytochemicals, that can effectively bind to them. This approach greatly minimizes the trial-and-error nature of traditional drug development by allowing precise predictions of compound-protein interactions. Key techniques in SBDD include molecular docking, which predicts the binding affinity and orientation of drug candidates targeting key protein; ADMET (absorption, distribution, metabolism, excretion, and toxicity) analysis, which assesses the pharmacokinetic and safety profiles of compounds; and molecular dynamics (MD) simulation, which evaluates the stability and flexibility of compound-receptor interactions over time. Additionally, DFT (Density functional theory)-based molecular reactivity analysis aids in understanding the electronic structure and kinetic stability of the lead compounds. Together, these methods streamline the drug discovery process, reducing time and costs, while enhancing the precision of selecting potential drug candidates from natural sources (Bajad *et al*., 2021; Ahmed *et al*., 2023a).

MMP-9 (Matrix Metalloproteinase-9) is a crucial enzyme involved in the degradation of the extracellular matrix (ECM), and plays a significant role in cancer progression, invasion, and metastasis across various types of cancers, including colorectal cancer (CRC) (Bendardaf *et al.*, 2010; Said *et al.*, 2014). MMP-9 is frequently overexpressed in CRC and is associated with poor prognosis due to its involvement in tumor growth, angiogenesis, and the spread of cancer cells to other tissues. Inhibiting MMP-9 has been suggested to reduce tumor invasiveness and slow metastasis, making it a viable target for therapeutic agents aimed at improving CRC outcomes (Rashid and Bardaweel, 2023; Sarkar *et al.*, 2024). Therefore, this MMP-9 protein serves as a promising target for structure-based drug design endeavors.

The study aims to identify, document, and analyze the angiosperm flora, particularly Liliopsida taxa of Rajbari district, assessing their current distribution, and medicinal significance. Consequently, it is crucial to identify, and document the plant species, providing a comprehensive taxonomic treatment of the angiosperm flora of Rajbari district, and to implement conservation measures to safeguard the region's plant resources for the benefit of future generations. In addition, the study further aims to bridge the gap between taxonomy and drug design endeavor by identifying potential colorectal cancer drug candidates targeting MMP-9 protein from a medicinal plant of Rajbari district. This multi-disciplinary endeavor, therefore aims not only to deepen the understanding of Liliopsida diversity in Rajbari district but also to investigate novel anticancer therapeutics derived from the selected medicinal plant.

Materials and Methods

Botanical expedition, plant sample collection and identification

A total of 128 field expeditions were conducted between 2019 to 2023 to collect plant specimens from Rajbari district covering all five upazilas: Rajbari Sadar, Pangsha, Baliakandi, Kalukhali and Goalanda (Fig. 1).

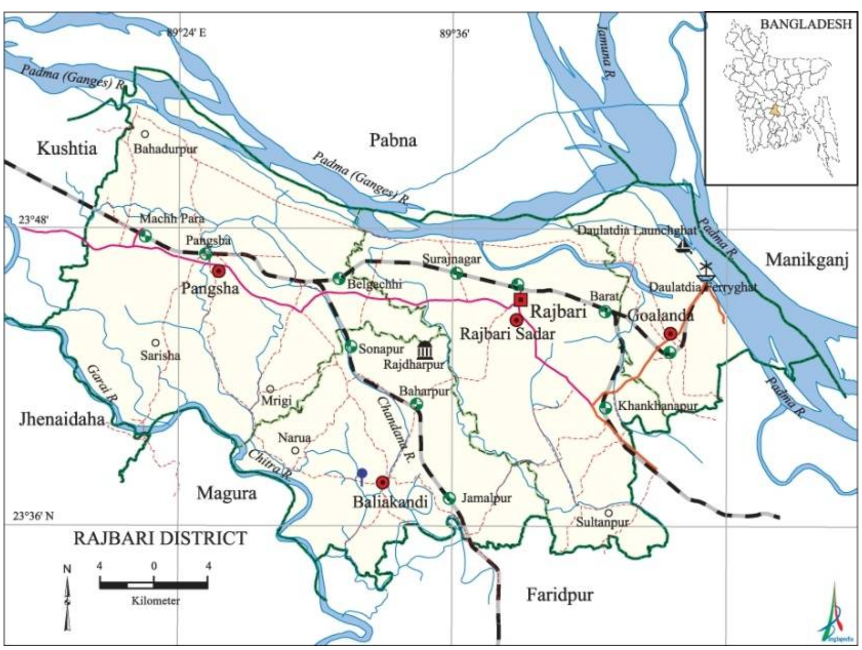

Fig. 1. Map of Rajbari district showing the area of investigation (Source: Banglapedia).

The collected plant samples were processed following standard herbarium procedures (Singh and Subramaniam, 2008) and underwent thorough examination and identification at the Dhaka University Salar Khan Herbarium (DUSH). Identifications were ensured by consulting standard literatures (Khan and Alam, 1977; Khan and Halim, 1985; Ara and Hassan, 2019; Siddiqui *et al*., 2007; Ahmed *et al*., 2008) and were cross-referenced with previously identified specimens housed at DUSH and DACB. For updated nomenclature, the authoritative database Plants of the World Online (POWO, 2024) was consulted. Local names were sourced from Huq (2019), and the families were arranged following Cronquist (1981). The voucher specimens for the identified taxa are deposited at DUSH.

Drug Design endeavor

Amorphophallus paeoniifolius (Dennst.) Nicolson was chosen for designing colorectal cancer drug candidates due to its novelty, ethnomedicinal significance, and consent of local population in the study area. The drug design endeavor was accomplished in the following steps:

Preparation of receptor macromolecule

The structure of the Matrix Metalloproteinase 9 (MMP-9) protein, identified by the PDB ID "1GKC," was retrieved from the Protein Data Bank (Rowsell *et al*., 2002). Receptor preparation was carried out using AutoDockTools v.1.5.6 and SWISS-PDB Viewer v.4.10. Subsequently, OpenBabel v.3.1.1.1 was employed to convert the energy-minimized protein from PDB to PDBQT format for further analysis (Guex and Peitsch, 1997; O'Boyle *et al*., 2008; Rizvi *et al*., 2013).

Preparation of ligands

Phytochemicals from *A. paeoniifolius* were identified and retrieved in 3D SDF format from relevant literature and the IMPPAT database (Shrivastava *et al*., 2023; Vivek-Ananth *et al*., 2023). Doxycycline, a known inhibitor of the MMP-9 receptor, was selected as the control drug and obtained from the PubChem database (Kim *et al*., 2005). All ligands were then energy-minimized and converted to PDBQT format using OpenBabel v.3.1.1.1 for further analysis.

Active site determination

For site-specific molecular docking, the receptor's active site was determined via the CASTp v.3.0 (Tian *et al*., 2018). The protein, uploaded in PDB format, was analyzed, and the active site with the highest surface area and volume was selected as the optimal site for docking simulations.

Molecular docking

A grid box for molecular docking was defined using the output from CASTp v.3.0, with dimensions of $68 \times 64 \times 66$ and center coordinates set to $61.125 \times 29.614 \times 113.283$ along the X, Y, and Z axes, respectively. Molecular docking was conducted using EasyDock Vina v.2.237 (Minibaeva *et al*., 2023). The receptor-ligand complexes were visualized with Discovery Studio (Islam *et al*., 2023). Following docking, the selected phytocompounds were evaluated through ADMET analysis for further assessment.

ADMET properties evaluation

The ADMET evaluation was performed using SwissADME to evaluate the drug-likeness of the compounds (Daina *et al*., 2017). Toxicity parameters were then analyzed using the STopTox server (Borba *et al*., 2022). For both analyses, the compounds were provided in SMILES format.

Molecular dynamics (MD) simulation

To examine the thermodynamic behavior of the control drug and lead compounds, molecular dynamics (MD) simulations were performed on an Ubuntu 22.04 (Jammy Jellyfish) operating system using the Desmond module of the Schrödinger 2020-1 package, over a duration of 100 ns (Rahman *et al.*, 2024). The simulated systems were solvated with the SPC water model in orthorhombic periodic boundary boxes. The OPLS4 force field was applied for energy optimization of the solvated framework, with the default settings in Desmond. Simulations were processed using the NPT ensemble, with Nose–Hoover temperature coupling and isotropic pressure scaling. The trajectories were sampled at 100 ps intervals, resulting in approximately 1000 frames for subsequent analysis, while energy data were recorded at 1.2 ps intervals.

Principal component analysis and Gibbs FEL

To analyze the essential dynamics of the top selected leads and the control drug, principal component analysis (PCA) was conducted using the Statistics Kingdom server (https://www.statskingdom.com/). RMSD and Rg coordinates for all simulated frames were input as two series to perform PCA using a covariance matrix. For Gibbs free energy landscape (FEL) analysis, a Python script was employed on Ubuntu Focal Fossa 20.04.6 LTS. The PCA data was saved in a CSV file for easy manipulation via the Pandas library. The script utilized essential libraries such as NumPy for numerical operations, facilitating the efficient computation of statistical metrics, and Matplotlib for data visualization. A 2D histogram of the PCA results was generated to estimate the probability distribution of data points, enabling the calculation of Gibbs free energy based on Boltzmann statistics (Ahmed and Rahman, 2024).

Molecular reactivity analysis

Quantum mechanics-based DFT calculation was performed to estimate molecular reactivity for the lead compounds and control drug employing Avogadro and ORCA v.4.1.1 software packages (Snyder and Kucukkal, 2021; Paul *et al.*, 2023). Input files were prepared in Avogadro for subsequent processing in ORCA. Geometry optimization was performed, employing the B3LYP-D3 functional and the 6-31G (d, p) basis set to estimate the HOMO-LUMO (Highest Occupied Molecular Orbital-Lowest Unoccupied Molecular Orbital) energy gap.

Results and Discussion

Angiosperm flora: Annotation of Liliopsida

The present study identified 201 taxa across 46 genera and 25 families within the class Liliopsida (monocotyledons) from Rajbari district (Table 1). Among the families, Poaceae emerged as the largest, comprising 58 taxa under 36 genera, followed by Araceae (26 species) and Cyperaceae (17 species). Figure 2 illustrates the ten largest families along with the number of genera and species. Agavaceae and Dioscoraceae each contribute 9 species, while the Liliaceae includes 8 species. The families Aponogetonaceae, Heliconiaceae, Lemnaceae, Orchidaceae, and Pontederiaceae each contain 3 species. Eight families, including Aloaceae, Cannaceae, Costaceae, Marantaceae, Musaceae, Smilacaceae, Strelitziaceae and Typhaceae are represented by a single species each. Among the genera, *Cyperus* stands out as the largest with 17 species, followed by *Dioscorea* with 10 species. The genera *Colocasia*, *Commelina* and *Digitaria* each contain 5 species, while *Alocasia, Bambusa, Eragrostis, Fimbristylis* and *Paspalum* are represented by 4 species each.

Vegetation analysis shows that the majority of the species are herbs, representing 79.6% (140 species) of the total, followed by climbers (7.96%), trees (7.46%), shrubs (2.98%), and epiphytes (1.99%). Habitat analysis reveals that fallow lands (open fields) constitute 24.38% of the identified species, followed by homestead (22.89%), scrub jungles (16.91%), agricultural fields (14.93%), aquatic (11.44%), and road sides (9.45%).

Table 1. List of Liliopsida taxa in Rajbari district with local name, habit, habitat, distribution and voucher numbers.

Taxa	Local name	Habit	Habitat	Distribution	Vouchers
Alismataceae					
Sagittaria guayanensis subsp. *lappula* (D. Don) Bogin	Muamia	Her	Aqu	Rs,Ka,Ba,Go,Pa	Miruna 1482
S. sagittifolia L.	Muamia	Her	Aqu	Rs,Ka,Ba,Go,Pa	Miruna 242
Hydrocharitaceae					
Hydrilla verticillata (L.f.) Royle	Kureli	Her	Aqu	Rs,Ka,Ba,Go,Pa	Miruna 2097
Nechamandra alternifolia (Roxb.) Thw.	Sheola	Her	Aqu	Rs,Ka,Ba,Go,Pa	Miruna 1749
Ottelia alismoides (L.) Pers.	Kuchkalai	Her	Aqu	Rs,Ka,Ba,Go,Pa	Miruna 1438
Vallisneria spiralis L.	Pata seola	Her	Aqu	Rs,Ka,Ba,Go,Pa	Miruna 1779
Aponogetonaceae					
Aponogeton appendiculatus Bruggen	Ghetu	Her	Aqu	Rs,Ba,Ka,Go,Pa	Miruna 185
Aponogeton crispus Thunb.	Ghechu	Her	Aqu	Rs,Ba,Ka,Go,Pa	Miruna 231
Aponogeton natans (L.) Engl. & Krause	Apanogeton	Her	Aqu	Rs,Ba,Ka,Go,Pa	Miruna 205
Arecaceae					
Areca catechu L.	Supari	Tre	Hom	Rs,Ka,Ba,Go,Pa	Miruna 1595
Borassus flabellifer L.	Tal	Tre	Roa	Rs,Ka,Ba,Go,Pa	Miruna 1673
Calamus viminalis Willd.	Bet	Cli	Scr	Rs,Ka,Ba,Go,Pa	Miruna 61
Caryota mitis Lour.	Bottle palm	Tre	Hom	Rs,Ka,Ba,Go,Pa	Miruna 1759
Caryota urens L.	Sagu palm	Tre	Hom	Rs,Ka,Ba,Go,Pa	Miruna 1663
Chrysalidocarpus lutescens (Bory) H. Wen.	Holud palm	Tre	Hom	Rs,Ba,Ka,Go,Pa	Miruna 1673
Cocos nucifera L.	Narikel	Tre	Hom	Rs,Ka,Ba,Go,Pa	Miruna 320
Corypha taliera Roxb.	Tali	Tre	Hom	Rs	Miruna 1449
Elaeis guineensis Jacq.	Oil Palm	Tre	Hom	Rs,Ka,Ba,Go,Pa	Miruna 1565
Licuala spinosa Wurmb	Unknown	Shr	Hom	Rs,Ka,Ba,Go,Pa	Miruna 1774
Phoenix sylvestris (L.) Roxb.	Khejur	Tre	Roa	Rs,Ka,Ba,Go,Pa	Miruna 1593
Araceae					
Adelonema wallisii (Regel) S.Y.Wong & Croat	Jongli kachu	Her	Scr	Rs,Go,Bal,Pa,Ka	Miruna 1015
Aglaonema costatum N.E. Brown	Nemacos	Her	Hom	Rs,Ka,Ba,Go,Pa	Miruna 1658
Aglaonema robeleynii (Van Geert) Pitcher & Manda	Nemacris	Her	Hom	Rs,Ka,Ba,Go,Pa	Miruna 1659
Alocasia cucullata (Lour.) G. Don	Bish kachu	Her	Scru	Rs,Ka,Ba,Go,Pa	Miruna 584
Alocasia fornicata (Roxb.) Schott	Salu kachu	Her	Hom	Rs,Ka,Ba,Go,Pa	Miruna 976
Alocasia macrorrhizos (L.) G. Don	Man kachu	Her	Scr	Rs,Ka,Ba,Go,Pa	Miruna 975
Alocasia portei Schott	Puti kachu	Her	Scr	Rs,Ka,Ba,Go,Pa	Miruna 977
Amorphophallus bulbifer (Schott) Blume	Jongle ol	Her	Scr	Rs,Ka,Ba,Go,Pa	Miruna 978
Amorphophallus paeoniifolius (Dennt.) Nicol.	Olkachu	Her	Agr	Rs,Ka	Miruna 586
Caladium bicolor (Ait.) Vent.	Diranga kachu	Her	Hom	Rs,Ka,Ba,Go,Pa	Miruna 979
Caladium humboldtii (Raf.) Schott	Befula kachu	Her	Hom	Rs,Ka,Ba,Go,Pa	Miruna 980
Colocasia esculenta (L.) Schott	Kachu	Her	Agr	Rs,Ka,Ba,Go,Pa	Miruna 981
Colocasia fallax Schott	Ranga kachu	Her	Hom	Rs,Ka,Ba,Go,Pa	Miruna 982
Colocasia mannii Hook. f.	Mani kachu	Her	Scr	Rs,Ka,Ba,Go,Pa	Miruna 1719
Epipremnum aureum (Linden & Andr.) G.S. Bunting	Pargacha	Cli	Roa	Rs,Go,Bal,Pa,Ka	Miruna 1723
Lasia spinosa (L.) Thw.	Kanta kachu	Her	Scru	Rs,Go,Bal,Pa,Ka	Miruna 329

Table 1 contd.

Taxa	Local name	Habit	Habitat	Distribution	Vouchers
Monstera obliqua Miq.	Thaka	Epi	Hom	Rs,Ka,Ba,Go,Pa	Miruna 1359
Pistia stratiotes L.	Topa pana	Her	Aqu	Ba,Go,Ka, Rs	Miruna 243
Raphidophora aurea (Linden & Andr.) Birdsey	Charulata	Cli	Roa	Ba,Go,Ka, Rs	Miruna 983
Scindapsus officinalis (Roxb.) Schott	Gaj pipal	Cli	Scr	Ka, Rs	Miruna 378
Scindapsus scortechinii Hook. f.	Kain kanthal	Cli	Scr	Ba,Rs	Miruna 994
Syngonium podophyllum Schott	Podolota kachu	Cli	Scr	Ba,Go,Ka,Rs,Pa	Miruna 984
Typhonium flagelliforme (Lodd.) Blume	Ghechu	Her	Scr	Ba,Go,Ka,Rs,Pa	Miruna 767
Typhonium roxburghii Schott	Roxy kachu	Her	Scr	Ba,Ka,Go,Rs,Pa	Miruna 774
Typhonium trilobatum (L.) Schott	Ghet kachu	Her	Scr	Rs,Ka,Ba,Go,Pa	Miruna 1594
Xanthosoma sagittifolium (L.) Schott	Dudh kachu	Her	Scr	Ra,Ka,Ba,Go,Pa	Miruna 1553
Lemnaceae					
Lemna minor L.	Kuti pana	Her	Aqu	Rs,Ka,Ba,Go,Pa	Miruna 670
Spirodela polyrhiza (L.) Schleid.	Tetule pana	Her	Aqu	Rs,Ka,Ba,Go,Pa	Miruna 244
Wolffia arrhiza (L.) Horkel *ex* Wimm.	Sujipana	Her	Aqu	Rs	Miruna 16
Commelinaceae					
Commelina appendiculata C.B. Clarke	Kulalatakansira	Her	Roa	Ba,Go,Ka, Rs	Miruna 1546
Commelina benghalensis L.	Kanshira	Her	Roa	Go,Ba,Ka,Rs	Miruna 382
Commelina erecta L.	Jata kansira	Her	Roa	Go,Ba,Ka,Rs	Miruna 1508
Commelina longifolia Lam.	Pani kansira	Her	Aqu	Ka,Go,Ba,Rs	Miruna 120
Commelina paludosa Blume	Kanchuria	Her	Roa	Ba,Go,Ka, Rs	Miruna 129
Cyanotis axillaris (L.) D. Don *ex* Sweet	Baghanula	Her	Roa	Ba,Go,Ka, Rs	Miruna 220
Cyanotis cristata (L.) D. Don	Unknown	Her	Roa	Go,Ka,Ba,Rs	Miruna 216
Floscopa scandens Lour.	Hangsapdi gac	Her	Roa	Rs,Go	Miruna 1504
Murdannia nudiflora (L.) Brenan	Kenduli	Her	Roa	Rs,Ka	Miruna 157
Tradescantia spathacea Sw.	Deopindo	Her	Hom	Rs,Ka,Ba,Go,Pa	Miruna 1521
Cyperaceae					
Actinoscirpus grossus (L.f.) Goetgh. & D.A. Simpson	Karui ghas	Her	Ope	Ra,Ka,Ba,Go,Pa	Miruna 1526
Bulbostylis barbata (Rottb.) C.B. Clarke	Bulbobata	Her	Ope	Rs,Ka,Ba,Go,Pa	Miruna 1763
Cyperus articulatus L.	Shoda	Her	Ope	Rs,Ka,Ba,Go,Pa	Miruna 1552
Cyperus fuscus L.	Kanch	Her	Ope	Rs,Ka,Ba,Go,Pa	Miruna 1295
Cyperus cuspidatus Kunth	Chapa ghas	Her	Ope	Rs,Ka,Ba,Go,Pa	Miruna 1577
Cyperus cyperoides (L.) Kuntze	Boro gothubi	Her	Agr	Rs,Ka,Ba,Go,Pa	Miruna 1509
Cyperus difformis L.	Behua	Her	Agr	Rs,Ka,Ba,Go,Pa	Miruna 83
Cyperus digitatus Roxb.	Hath ghas	Her	Ope	Rs,Ba	Miruna 1296
Cyperus exaltatus Retz.	Tata ghas	Her	Aqu	Rs,Pa,Go	Miruna 1510
Cyperus imbricatus Retz.	Buethi	Her	Ope	Rs,Pa,Go,	Miruna 1520
Cyperus iria L.	Barachucha	Her	Ope	Ra,Ka,Ba,Go,Pa	Miruna 1483
Cyperus michelianus (L.) Delile	Choto gutubi	Her	Ope	Rs,Ka,Ba,Go,Pa	Miruna 1572
Cyperus mindorensis (Steud.) Huygh	Gothubi	Her	Agr	Rs,Ka,Ba,Go,Pa	Miruna 1862
Cyperus procerus Rottb.	Lamba mutha	Her	Ope	Rs,Ka,Ba,Go,Pa	Miruna 199
Cyperus pulcherrimus Willd. *ex* Kunth	Shumo mutha	Her	Ope	Rs,Ka,Ba,Go,Pa	Miruna 1294
Cyperus pumilus L.	Paikpami ghas	Her	Agr	Rs,Ka,Ba,Go,Pa	Miruna 1740
Cyperus rotundus L.	Mutha	He	Ope	Ra,Ka,Ba,Go,Pa	Miruna 214

Table 1 contd.

Taxa	Local name	Habit	Habitat	Distribution	Vouchers
Cyperus tenuiculmis Boeck.	Khude potari	Her	Ope	Rs,Ka,Ba,Go,Pa	Miruna 1484
Cyperus thunbergii Vahl	Mura ghas	Her	Ope	Ra,Ka,Ba,Go,Pa	Miruna 1548
Cyperus tuberosus Rottb.	Dima mutha	Her	Ope	Rs,Ka,Ba,Go,Pa	Miruna 1291
Eleocharis acutangula (Roxb.) Schult.	Chesra	Her	Ope	Rs,Go	Miruna 1837
Fimbristylis aestivalis (Retz.) Vahl	Valis fibri	Her	Ope	Rs,Ka,Ba,Go,Pa	Miruna 148
Fimbristylis alboviridis C.B. Clarke	Sadate fimbri	Her	Ope	Rs,Ka,Ba,Go,Pa	Miruna 373
Fimbristylis dichotoma (L.) Vahl subsp. *dichotoma*	Bara nirbishi	Her	Agr	Rs,Ka,Ba,Go,Pa	Miruna 123
Fimbristylis miliacea (L.) Vahl	Bura javani	Her	Ag	Rs,Ka,Ba,Go,Pa	Miruna 142
Fuirena ciliaris (L.) Roxb.	Chhata ghas	Her	Agr	Rs,Ka,Ba,Go,Pa	Miruna 1800
Rhynchospora berteroi (Spreng.) C.B. Clarke	Bindimuthi	Her	Ope	Rs,Ka,Ba,Go,Pa	Miruna 1826
Schoenoplectiella supina (L.) Lye	Putputicechra	Her	Agr	Ra,Ka,Ba,Go,Pa	Miruna 190
Poaceae					
Alloteropsis cimicina (L.) Stapf	Alotara cina	Her	Ope	Rs,Go	Miruna 1564
Avena fatua L.	Jangli jai	Her	Aqu	Rs,Pa	Miruna 1396
Axonopus compressus (Sw.) P. Beauv.	Mathghas	Her	Ope	Go,Ka,Ba,Rs	Miruna 1527
Bambusa balcooa Roxb.	Baro aansh	Tre	Scr	Ba,Ka,Go,Rs	Miruna 1551
Bambusa bambos (L.) Voss	Bon bans	Tre	Scr	Ka,Ba,Go, Rs	Miruna 1561
Bambusa salarkhanii M. K. Alam	Katajali bans	Tre	Scr	Rs	Miruna 687
Bambusa vulgaris Scharad. *ex* Wendl.	Jai bansh	Tre	Hom	Ra,Ka,Ba,Go	Miruna 1834
Bothriochloa bladhii (Retz.) S. T. Blake	Gandagourana	Her	Hom	Rs,Ka,Ba,Go,Pa	Miruna 2011
Bothriochloa pertusa (L.) A. Camus	Barmuda ghas	Her	Ope	Ra,Ka,Ba,Go,Pa	Miruna 2093
Cenchrus purpureus (Schumach.) Morrone	Nepier ghas	Her	Ope	Rs,Ka,Ba,Go	Miruna 717
Chrysopogon aciculatus (Retz.) Trin.	Chorkanta	Her	Ope	Rs,Ka,Ba,Go	Miruna 1761
Coix aquatica Roxb.	Tosbi dana	Her	Agr	Rs, Go	Miruna 487
Cynodon dactylon (L.) Pers.	Durba ghas	Her	Ope	Go,Ba,Ka,Rs	Miruna 605
Cyrtococcum accrescens (Trin.) Stapf	Konaghas	Her	Ope	Go,Ba,Ka,Rs	Miruna 520
Cyrtococcum oxyphyllum (Hochst. *ex* Steud.) Stapf	Pokra ghas	Her	Ope	Go,Ba,Ka,Rs	Miruna 521
Dactyloctenium aegyptium (L.) Willd.	Mukra	Her	Ope	Rs,Go,Ba,Pa,Ka	Miruna 118
Desmostachya bipinnata (L.) Stapf	Kusha	Her	Ope	Rs,Ka,Ba,Go,Pa	Miruna 1821
Digitaria ciliaris (Retz.) Koeler	Kokjachira	Her	Ope	Rs,Ka,Ba,Go,Pa	Miruna 172
Digitaria ischaemum (Schreb.) Muhl.	Kudeanguligas	Her	Ope	Rs,Ka,Ba,Go,Pa	Miruna 519
Digitaria sanguinalis (L.) Scop.	Makunjali	Her	Roa	Rs,Ka,Ba,Go,Pa	Miruna 518
Digitaria setigera Roth	Sheti ghas	Her	Roa	Rs,Ka,Ba,Go,Pa	Miruna 517
Digitaria ternata (A. Rich.) Stapf	Nata ghas	Her	Agr	Rs,Ka,Ba,Go,Pa	Miruna 516
Dinebra chinensis (L.) Peterson & N.Snow	Phulka ghas	Her	Agri	Ba,Go,Ka,Rs,Pa	Miruna 124
Echinochloa colonum (L.) Link	Shama ghas	Her	Agr	Ba,Go,Ka,Rs	Miruna 177
Echinochloa crus-galli (L.) P. Beauv.	Borosama ghas	Her	Agr	Ba,Go,Ka,Rs	Miruna 133
Eleusine indica (L.) Gaertn.	Ghira durba	Her	Agr	Ba,Go,Ka,Rs	Miruna 122
Eragrostis japonica (Thunb.) Trin.	Chira ghas	Her	Agri	Ba,Go,Ka,Rs	Miruna 1529
Eragrostis lehmanniana Nees	Kona ghas	Her	Ope	Ba,Go,Ka,Rs	Miruna 1559
Eragrostis tenella (L.) P. Beauv. *ex* Roem. & Schult.	Koni ghas	Her	Ope	Ba,Go,Ka,Rs	Miruna 208
Eragrostis unioloides (Retz.) Nees *ex* Sted.	Chiraghas	Her	Ope	Ba,Ka,Go,Rs	Miruna 178
Hemarthria protensa Steud.	Panseru	Her	Ope	Rs,Go	Miruna 200

Table 1 contd.

Taxa	Local name	Habit	Habitat	Distribution	Vouchers
Hordeum vulgare L.	Job	Her	Agr	Go,Ba,Rs,Ka	Miruna 1515
Imperata cylindrica var. *latifolia* (Hook. f.) C. E. Hubb.	Chon	Her	Ope	Go,Ba,Rs,Ka	Miruna 1525
Imperata cylindrica var. *major* (Nees) C. E. Hubb. *ex* Hubb. & Vaughan	Kash	Her	Ope	Ra,Ka,Ba,Go	Miruna 202
Leersia hexandra Sw.	Arali Ghas	Her	Ope	Ba,Go,Ka,Rs,Pa	Miruna 1524
Louisiella paludosa (Roxb.) Landge	Barti	Herb	Aqu	Rs,Ka,Ba,Go,Pa	Miruna 512
Melocanna baccifera (Roxb.) Kurz	Muli Bansh	Shr	Hom	Rs,Ba, Ka,Go,Pa	Miruna 2026
Oplismenus burmanni (Retz.) P. Beauv.	Jabri durba	Her	Roa	Rs,Ka,Ba,Go,Pa	Miruna 207
Oryza sativa L.	Dhan	Her	Agr	Rs,Ka,Go,BaPa	Miruna 1068
Panicum brevifolium L.	Panibrevi ghas	Her	Ope	Rs,Ba,Go,Pa, Ka	Miruna 513
Panicum miliaceum L.	Cheena chaul	Her	Agr	Rs,Pa	Miruna 1581
Paspalum conjugatum Bergius	Dadkuru	Herb	Ope	Rs,Ka,Ba,Go,Pa	Miruna 511
Paspalum distichum L.	Nat ghas	Herb	Aqu	Rs,Go,Pa	Miruna 150
Paspalum scrobiculatum L.	Goicha	Herb	Ope	Rs, Bal,Ka	Miruna 1774
Paspalum sumatrense Roth	Lambafuli ghas	Herb	Ope	Pa,Go,	Miruna 1757
Pennisetum purpureum Schum.	Hati ghas	Herb	Ope	Ba,Rs,Go,Pa	Miruna 1841
Saccharum officinarum L.	Akh	Shrub	Agr	Ba,Go,Rs,Ka	Miruna 423
Saccharum spontaneum L.	Kash	Herb	Ope	Ba,Ka,Go, Rs	Miruna 524
Setaria flavida (Retz.) Veldkamp	Datkuri ghas	Herb	Roa	Rs,Ka,Ba,Go,Pa	Miruna 1775
Setaria pumila (Poir.) Roem. & Schult.	Holde kaon	Herb	Ope	Rs,Pa,Ka,Ba,Go	Miruna 524
Sporobolus indicus R. Br.	Ghas	Herb	Ope	Rs,Pa,Ka,Ba,Go	Miruna 337
Thyrsostachys oliveri Gamble	Burma bans	Tree	Ope	Rs,Pa,Ka,Ba,Go	Miruna 1453
Triticum aestivum L.	Gom	Herb	Agr	Ba,Go,Ka,Pa,Rs	Miruna 1693
Urochloa panicoides P. Beauv.	Ghas	Herb	Ope	Rs,Ka,Ba,Go,Pa	Miruna 1713
Urochloa ramosa (L.) T.Q.Nguyen	Jhopa ghas	Her	Agri	Rs,Ka,Ba,Go,Pa	Miruna 1903
Urochloa reptans (L.) Stapf	Para ghas	Her	Ope	Rs,Ka,Ba,Go,Pa	Miruna 205
Urochloa setigera (Retz.) Stapf	Baro goghonti	Her	Ope	Rs,Go	Miruna 1769
Zea mays L.	Bhutta	Herb	Agr	Rs,Ka,Ba,Go,Pa	Miruna 1664
Typhaceae					
Typha elephantina Roxb.	Hogla	Herb	Aqu	Ka, Rs	Miruna 1048
Strelitziaceae					
Ravenala madagascariensis Sonn.	Panthopadop	Tre	Hom	Go,Rs,Ka,Pa,Ba	Miruna 1691
Heliconiaceae					
Heliconia humilis Jacq.	Tiapakhi phul	Her	Hom	Go,Pa,Rs,Ka,Ba	Miruna 1446
Heliconia psittacorum L. f.	Tia thuti	Her	Hom	Go,Pa,Rs,Ka,Ba	Miruna 1467
Heliconia rostrata Ruiz & Pavon	Chingri nomi	Her	Hom	Rs,Go Ka,Ba,Pa	Miruna 390
Musaceae					
Musa paradisiaca L.	Kanch kola	Her	Hom	Rs,Go Ka,Ba,Pa	Miruna 389
Zingiberaceae					
Alpinia nigra (Gaertn.) Burtt	Tara	Her	Scr	Rs,Go,Ka	Miruna 941
Curcuma amada Roxb.	Amada	Her	Scr	Rs	Miruna 458
Curcuma longa L.	Halud	Her	Agr	Ba,Ka,Go,Pa,Rs	Miruna 1597
Curcuma zedoaria (Christm.) Rosc.	Shati	Her	Agr	Rs,Ba,Ka	Miruna 1687
Elettaria cardamomum (L.) Maton	Elach	Her	Agr	Rs	Miruna 606
Hedychium coronarium Koen.	Dolonchapa	Her	Hom	Rs,Go,Ba,Pa,Ka	Miruna 1690

Table 1 contd.

Taxa	Local name	Habit	Habitat	Distribution	Vouchers
Kaempferia galanga L.	Ekangi	Her	Hom	Ba,Rs,Ka	Miruna 456
Zingiber montanum (Koen.) Dietr.	Bon ada	Her	Scr	Ka,Rs,Ba	Miruna 1691
Zingiber officinale Rosc.	Ada	Her	Agr	Go,Ba,Pa,Rs,Ka	Miruna 457
Zingiber zerumbet (L.) Roscoe *ex* Sm.	Shoti	Her	Scr	Ka, Rs	Miruna 638
Costaceae					
Hellenia speciosa (J. Koenig) S.R. Dutta	Kura	Her	Hom	Ba,Ka,Go,Pa,Rs	Miruna 369
Cannaceae					
Canna indica L.	Kolaboti	Her	Hom	Ba,Pa,Rs,Ka,Go	Miruna 439
Marantaceae					
Schumannianthus benthamianus (Kuntze) Veldkamp & Turner	Shitolpati	Her	Aqu	Rs,Go	Miruna 388
Pontederiaceae					
Pontederia crassipes Mart.	Kachuripana	Her	Aqu	Go,Rs,Ba,Pa,Ka	Miruna 685
Pontederia hastata L.	Baranukha	Her	Aqu	Pa,Rs,Ka,Go,Ba	Miruna 822
Pontederia vaginalis Burm. f.	Nukha	Her	Aqu	Go,Rs,Ba,Pa,Ka	Miruna 1124
Liliaceae					
Allium cepa L.	Piaj	Her	Agr	Rs,Ba,Go,Ka	Miruna 425
Allium sativum L.	Rasun	Her	Agr	Rs,Go,Ka,Ba	Miruna 583
Asparagus racemosus Willd.	Shatomuli	Cli	Hom	Rs,Go,Ba	Miruna 589
Crinum asiaticum L.	Shukhdorson	Her	Hom	Pa,Rs,Ka,Go,Ba	Miruna 1528
Pancratium verecundum Ait.	Goroshun	Her	Scr	Go,Rs,Ka	Miruna 1248
Scadoxus multiflorus (Martyn) Raf.	Ball phul	Her	Hom	Pa,Rs,Ka,Go,Ba	Miruna 1568
Zephyranthes minuta (Kunth) D. Dietr.	Golapi ghasful	Her	Hom	Go,Pa,Ka,Rs,Ba	Miruna 1579
Zephyranthes tubispatha (L'Hér.) Herb.	Holud ghasful	Her	Hom	Go,Pa,Ka,Rs,Ba	Miruna 1542
Aloeaceae					
Aloe vera (L.) Burm. f.	Ghritakumari	Her	Hom	Rs,Ka,Go,Ba	Miruna 940
Agavaceae					
Agave americana L.	Cantala	Her	Hom	Rs,Ka,Go,Ba	Miruna 1522
Agave amica (Medik.) Thiede & Govaerts	Rajanigandha	Her	Hom	Rs,Ka,Go,Ba	Miruna 1447
Agave sisalana Perrine	Sisal hemp	Her	Hom	Rs,Ka,Go,Ba	Miruna 1570
Agave vivipara L.	Bombai agar	Her	Hom	Rs,Ka,Ba,Go	Miruna 1590
Cordyline fruticosa (L.) A. Chev.	Agnishar	Shr	Hom	Ba,Rs,Ka,Go	Miruna 1617
Dracaena angustifolia (Medik.) Roxb.	Chikna drakan	Shr	Hom	Rs,Ka,Go,Ba	Miruna 1501
Dracaena trifasciata (Prain) Mabb.	Gora chaka	Her	Hom	Rs,Ka,Go,Ba	Miruna 1657
Furcraea foetida (L.) Haw.	Gandho hemp	Shr	Hom	Rs,Ka,Go,Ba	Miruna 1672
Sansevieria roxburghiana Schult. & Schult.f.	Gora chaka	Her	Hom	Rs,Ka,Go,Ba	Miruna 1448
Smilacaceae					
Smilax perfoliata Lour.	Kumarilata	Cli	Scr	Go,Ba,Rs,Ka	Miruna 326
Dioscoreaceae					
Dioscorea aculeata L.	Jointia alu	Her	Scr	Rs,Ka,Go,Ba	Miruna 558
Dioscorea alata L.	Chupri alu	Cli	Scr	Rs,Ka,Go,Ba	Miruna 126
Dioscorea belophylla (Prain) Voigt *ex* Hai.	Shora alu	Cli	Scr	Rs,Ka,Go,Ba	Miruna 1540
Dioscorea bulbifera var. *bulbifera* L.	Gonj alu	Cli	Scr	Rs,Ka,Go,Ba	Miruna 449
Dioscorea bulbifera var. *sativa* Prain	Jen alu	Cli	Roa	Rs,Ka,Go,Ba	Miruna 559
Dioscorea esculenta (Lour.) Burkill	Maitta alu	Cli	Roa	Rs,Ka,Go,Ba	Miruna 451

Table 1 contd.

Taxa	Local name	Habit	Habitat	Distribution	Vouchers
Dioscorea kamoonensis Kunth	Erabera lata	Cli	Roa	Rs,Ka,Go,Ba	Miruna 125
Dioscorea oppositifolia L.	Ludi korphul	Cli	Scr	Rs,Ka,Go,Ba	Miruna 560
Dioscorea pentaphylla L.	Jhum alu	Cli	Scr	Rs,Ka,Go,Ba	Miruna 155
Orchidaceae					
Acampe praemorsa var. *longepedunculata* (Trimen) Govaerts	Pargacha	Epi	Scr	Go,Rs,Ba,Pa,Ka	Miruna 1823
Rhynchostylis retusa (L.) Blume	Rasna	Epi	Scr	Go,Rs,Ba,Pa,Ka	Miruna 1840
Vanda tessellata (Roxb.) Hook. *ex* G. Don	Pargacha	Epi	Scr	Go,Rs,Ba,Pa,Ka	Miruna 1828

Habit: Her: Herb, Shr: Shrub, Tre: Tree, Cli: Climber, Epi: Epiphyte; **Habitat**: Aqu: Aquatic, Scr: Scrub jungles, Roa: Roadside, Hom: Homestead, Agr: Agricultural field, Ope: Open field; **Distribution**; Rs: Rajbari sadar, Ba: Baliakandi, Go: Goalondo, Ka: Kalukhali, Pa: Pangsha.

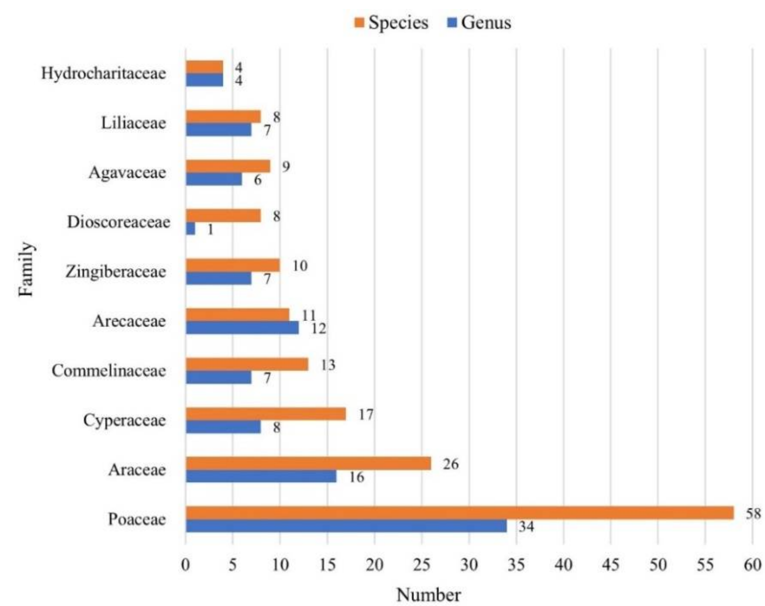

Fig. 2. Ten dominant families of Liliopsida illustrating the number of genera and species in Rajbari.

The study area supports a variety of aquatic habitats including ponds, beels, lowlands, and rivers, where many monocot species are found, and some of the common aquatic species are *Aponogeton appendiculatus*, *Aponogeton natans*, *Eichhornia crassipes*, *Hydrilla verticillata*, *Ottelia alismoides*, *Pistia stratiotes*, *Sagittaria sagittifolia*, *Typha elephantina*, *Vallisneria spiralis*, *Wolffia arrhiza* etc. A total of 25 medicinal plants used by traditional healers in the study area for treatment of different diseases, and notable species are *Aloe vera*, *Amorphophallus paeoniifolius*, *Colocasia esculenta*, *Hellenia speciosa*, *Curcuma amada*, *Cyperus rotundus*, *Dioscorea alata*, *Kaempferia galanga*, *Lasia spinosa*, *Pontederia hastata*, *Vanda tessellata* and *Zingiber zerumbet*. Some medicinally important and rare species are shown in Figure 3. Field observations have identified several rare species, such as *Coix aquatica*, *Schumannianthus benthamianus*, *Bulbostylis barbata* and *Bambusa salarkhanii*, which warrants further attention for conservation efforts.

While numerous studies have focused on the angiosperm flora of several upazilas in Bangladesh (Islam *et al*., 2009; Rahman *et al*., 2019a,b; Sarker *et al*., 2013; Sajib *et al*., 2014; Mahmudah *et al*., 2017), little effort has been made to produce comprehensive district-level flora. Khanam and Khan (2020) documented 168 species of Liliopsida (monocotyledons) from Narsinghdi district, whereas Hossain *et al.* (2021) identified 144 taxa from Liliopsida in the coastal district Satkhira, and Islam *et al.* (2022) reported a mere 133 taxa from Borguna district. In contrast, higher numbers of monocotyledonous taxa were recorded in Chapai Nawabganj and Rangpur districts, with 224 and 211 taxa, respectively (Islam and Khan, 2024; Khan *et al*., 2021).

Fig. 3. Some medicinal and rare plants of Rajbari district. A. *Amorphophallus paeoniifolius*, B. *Bambusa salarkhanii,* C. *Corypha taliera,* D. *Curcuma amada,* E. *Cyanotis cristata,* F. *Cyperus michelianus,* G. *Cyrtococcum accrescens,* H. *Dactyloctenium aegyptium,* I. *Heliconia rostrata,* J. *Hellenia speciosa,* K. *Kaempferia galanga,* L. *Nechamandra alternifolia,* M. *Pontederia hastata,* N. *Schumannianthus benthamianus*, O. *Syngonium podophyllum,* P. *Zingiber zerumbet.*

Compared to the earlier reports, our study, with 201 monocotyledonous taxa from Rajbari, surpasses the figures reported for Narsinghdi, Borguna, Satkhira, and Patuakhali (Sultana, 2012; Khanam and Khan, 2020; Hossain *et al*., 2021; Islam *et al*., 2022), yet falls slightly short compared to the monocot floras of Rangpur and Chapai Nawabganj flora (Khan *et al*., 2021; Islam and Khan, 2024).

Molecular docking analysis

A total of 27 unique active site residues were identified in the MMP-9 receptor (Fig. 4). The surface area (SA) was calculated as 205.130 Å², with a volume of 102.572 Å³, making the active site as a significant binding region for molecular docking analysis. Performing site-specific docking with active site residues is crucial in accurately predicting the binding interactions between ligands and their target proteins. Unlike blind docking, which assesses potential binding across the entire protein surface, site-specific docking focuses on predefined active sites, enhancing the precision of ligand placement. This targeted approach allows for a more refined understanding of ligand-receptor interactions, increasing the likelihood of identifying effective drug candidates (Ahmed and Rahman, 2024).

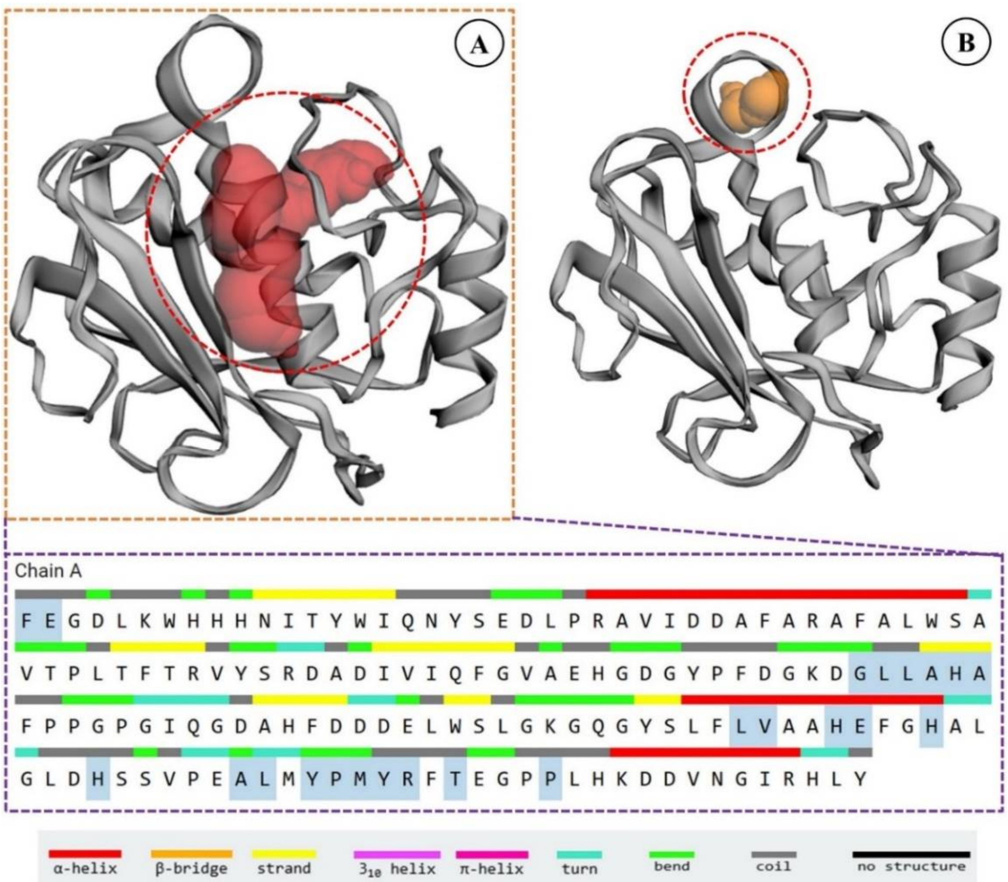

Fig. 4. Determination of the best ranked binding site in MMP-9 receptor. Rank 1 cavity was determined as the final binding site for its highest surface area and volumetric features. A. Rank 1 cavity, B. Rank 2 cavity.

Molecular docking of 22 phytocompounds of *A. paeoniifolius* revealed binding affinity ranged from -4.1 to -8.1 kcal/mol (Table 2). Alpha-carotene showed the highest affinity (-8.1 kcal/mol), while Oxalic acid demonstrated the lowest affinity (-4.1 kcal/mol). Doxycycline, as a control, scored -6.0 kcal/mol and comparing with it, a total of nine phytocompounds scored better than the control. These nine compounds were put forward for second-step screening via ADMET assay that revealed two lead compounds such as Riboflavin and Lupeol. The docked complexes of the leads and control drug are visualized in the Figure 5.

Table 2. Binding affinities of *A. paeoniifolius* phytocompounds against the receptor MMP-9.

No.	Ligands	IMPAAT ID/ PubChem CID	Chemical formula	Molecular weight (g/mol)	Binding affinity (kcal/mol)
1	Alpha-carotene	IMPHY011609	$C_{40}H_{56}$	536.9	-8.1
2	**Riboflavin**	IMPHY000846	$C_{17}H_{20}N_4O_6$	376.4	**-7.9**
3	Stigmasterol	IMPHY014842	$C_{29}H_{48}O$	412.7	-7.6
4	Quercetin	IMPHY004619	$C_{15}H_{10}O_7$	302.2	-7.2
5	Beta-sitosterol	IMPHY014836	$C_{29}H_{50}O$	414.7	-6.9
6	Retinol	IMPHY001308	$C_{20}H_{30}O$	286.5	-6.3
7	Amylotetraose	IMPHY008888	$C_{24}H_{42}O_{21}$	666.6	-6.3
8	Betulinic acid	IMPHY012003	$C_{30}H_{48}O_3$	456.7	-6.1
9	**Lupeol**	IMPHY012473	$C_{30}H_{50}O$	426.7	**-6.1**
10	1-ethoxy-4-[(Z)-2-nitroprop-1-enyl] benzene	5373673	$C_{11}H_{13}NO_3$	207.2	-5.9
11	Palmitic acid	IMPHY007327	$C_{16}H_{32}O_2$	256.4	-5.9
12	D-xylose	IMPHY015116	$C_5H_{10}O_5$	150.1	-5.9
13	4,6-Di-tert-butylresorcinol	79337	$C_{14}H_{22}O_2$	222.3	-5.7
14	D-galactose	IMPHY012050	$C_6H_{12}O_6$	180.1	-5.7
15	Nicotinic acid	IMPHY007357	$C_6H_5NO_2$	123.1	-5.6
16	L-rhamnose	IMPHY015056	$C_6H_{12}O_5$	164.1	-5.6
17	Thiamine	IMPHY000005	$C_{12}H_{17}N_4OS^+$	265.3	-5.5
18	Phytic acid	IMPHY007365	$C_6H_{18}O_{24}P_6$	660.0	-5.5
19	Beta-sitosterol palmitate	IMPHY003933	$C_{45}H_{80}O_2$	653.1	-5.4
20	Triacontane	IMPHY009413	$C_{30}H_{62}$	422.8	-5.0
21	Calcium oxalate	IMPHY003530	C_2CaO_4	128.1	-4.2
22	Oxalic acid	IMPHY007450	$C_2H_2O_4$	90.0	-4.1
23	Doxycycline (control)	54671203	$C_{22}H_{24}N_2O_8$	444.4	-6.0

Molecular interaction analysis

The molecular interaction study revealed similar interaction patterns between the lead compounds and Doxycycline. Among the two leads and control, conventional hydrogen bonds (CHBs) were observed only in Riboflavin, supporting its superiority as potential anticancer drug candidate (Table 3). Riboflavin interacted with residues Gly186, Leu187, Leu188, His401, Glu402, His405, His411 and Met422 (Fig. 6A), forming CHBs with Gly186 and Met422 residues, while other residues were involved in hydrophobic interactions. Lupeol showed interactions with Leu187, Leu188, His401, His411, and Pro421 residues (Fig. 6B) where all residues formed hydrophobic interactions. Doxycycline interacted with Phe110, Leu187, His190, and His411 residues with hydrophobic bonding only (Fig. 6C). Hydrogen bonding and hydrophobic interactions are very important for drug binding and efficacy. Hydrogen bonds stabilize ligand-receptor complexes, enhancing specificity and orientation, which improves binding affinity.

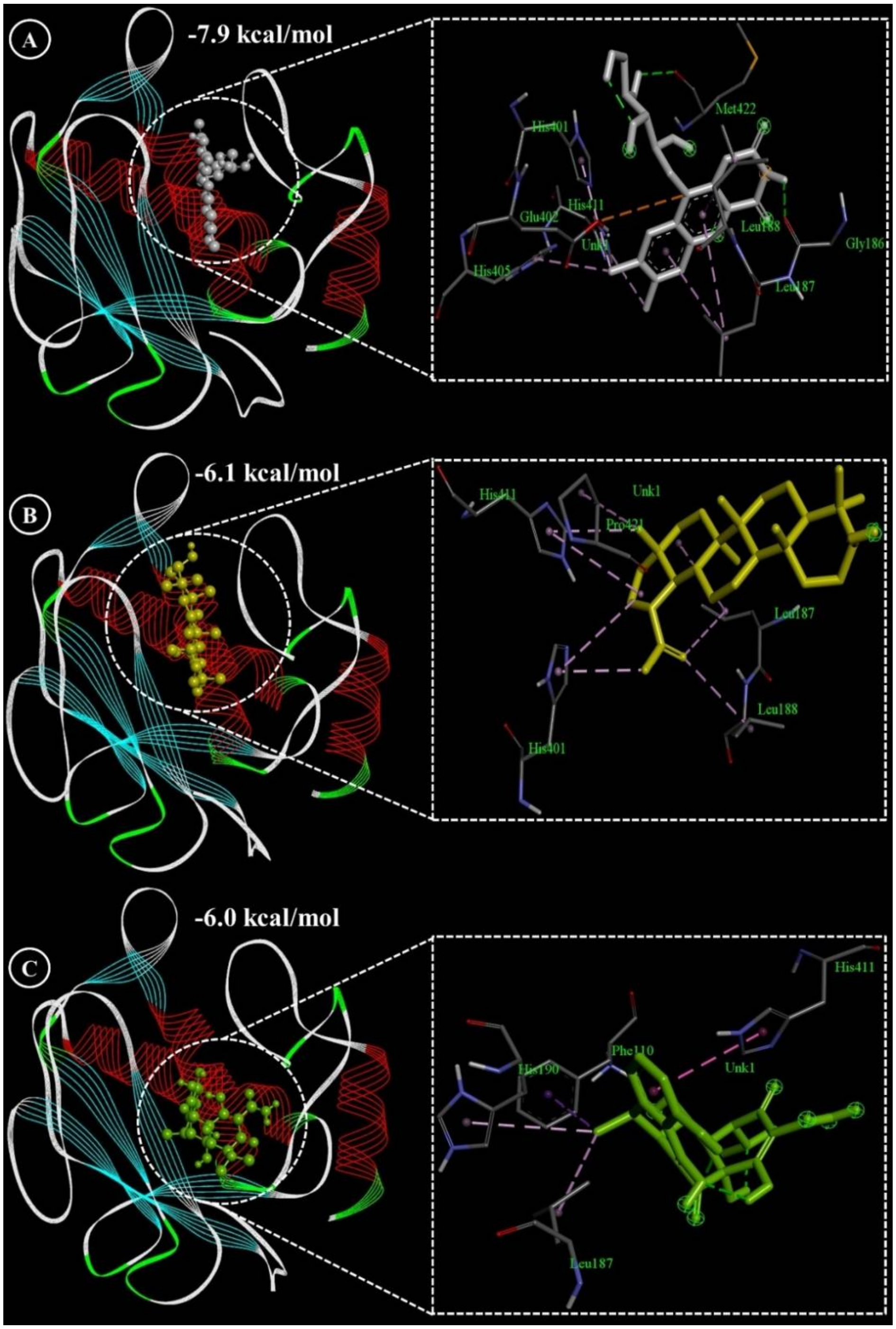

Fig. 5. Two lead compounds and control drug showing docked complexes after molecular docking analysis. A. Riboflavin, B. Lupeol, C. Doxycycline (control).

These interactions often dictate the orientation of the ligand within the binding cavity, facilitating effective biological activity. On the contrary, hydrophobic interactions promote the exclusion of water molecules from the binding site, further increasing the stability of the ligand-receptor complex. These interactions occur between nonpolar residues and contribute significantly to the overall binding energy (Ahmed *et al.*, 2023b).

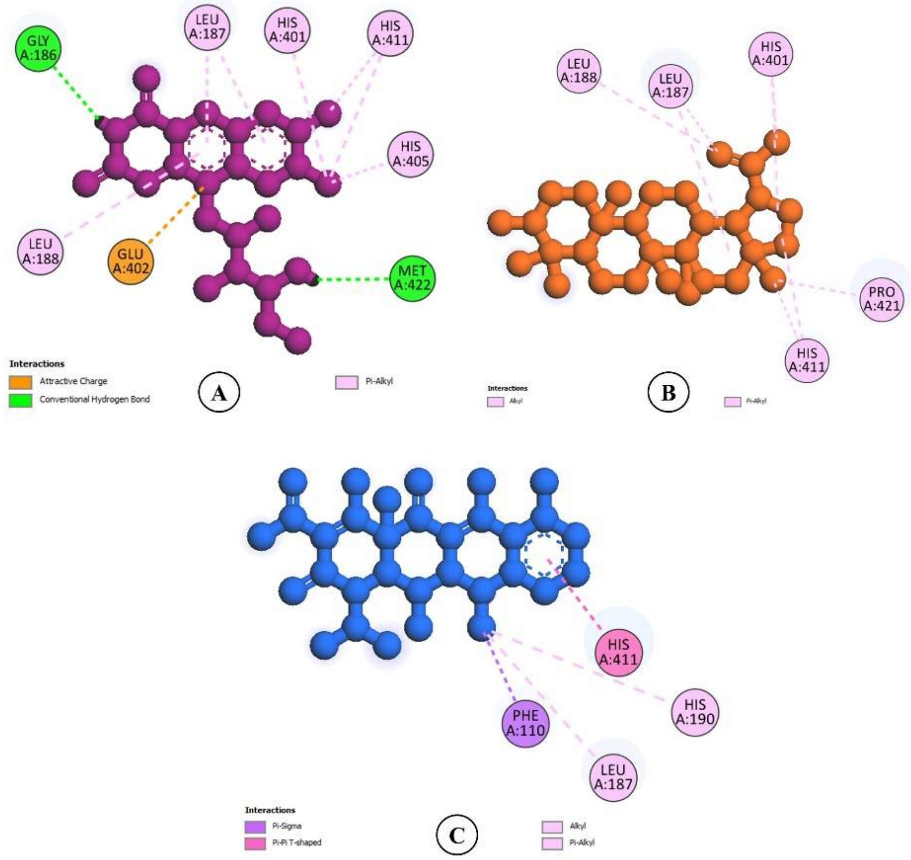

Fig. 6. Two-dimensional molecular interaction analysis of the two leads and control drug targeting MMP-9 protein. A. Riboflavin, B. Lupeol, C. Doxycycline.

Table 3. Evaluation of molecular interaction between the leads and the control drug targeting MMP-9 protein.

Ligands	Binding sites	Hydrogen-bonding residues (Distance in Å)	Hydrogen bonds number	Hydrophobic-interaction	Binding affinity (kcal/mol)
Riboflavin	Gly186, Leu187, Leu188, His401, Glu402, His405, His411, Met422	Gly186$^{(2.54)}$, Met422$^{(2.59)}$	2	Leu187, Leu188, His401, Glu402, His405, His411	-7.9
Lupeol	Leu187, Leu188, His401, His411, Pro421	No residues	0	Leu187, Leu188, His401, His411, Pro421	-6.1
Doxycycline (control)	Phe110, Leu187, His190, His411	No residues	0	Phe110, Leu187, His190, His411	-6.0

ADMET evaluation

ADMET study revealed drug-likeness of Riboflavin and Lupeol in comparison with Doxycycline (Table 4, Fig. 7). Among the lead compounds, Lupeol exhibited the highest molecular weight (426.7 g/mol). The H-bond accepting and donating profiles of Riboflavin was closely comparable to those of Doxycycline, while Lupeol demonstrated only one H-bond donor and acceptor. Lupeol had the highest molar refractivity score, while Riboflavin had the lowest. TPSA was lowest for Lupeol, while it was highest for Doxycycline. The gastrointestinal absorption capacity of the two lead compounds were very similar to that of the control drug. The CYP isoform inhibition profiles of both leads and Doxycycline were alike, with none showing inhibition against various CYP isoforms (Table 4). In terms of solubility, Riboflavin was highly soluble, Doxycycline was soluble and Lupeol exhibited poor solubility. Riboflavin adhered to Lipinski's rule of five with zero violation, while Lupeol and Doxycycline demonstrated one violation each which is acceptable. In toxicity analysis, Riboflavin and Lupeol revealed satisfactory results with no major undesirable complications, similar to the control drug Doxycycline. The ADMET results of the present investigation were consistent with previous SBDD studies (Rahman *et al.*, 2024; Ahmed *et al*., 2023a,b; Ahmed *et al*., 2024).

Fig. 7. Drug-likeness and oral bioavailability evaluation of the leads and Doxycycline. LIPO indicates lipophilicity, INSOLU depicts insolubility, INSATU suggests insaturation index, FLEX points flexibility, SIZE implies molecular weight, and POLAR denotes polarity. Pink region reflects the best zone while red line denotes best fit. A. Riboflavin, B. Lupeol, C. Doxycycline.

Molecular dynamics simulation

The MD simulation analysis unveiled structural stability and compactness of Riboflavin and Lupeol (Table 5). Both the leads showed similar mean values in RMSD (root mean square deviation), RMSF (root mean square fluctuation), Rg (radius of gyration), and SASA (solvent accessible surface area). The RMSD analysis showcased the stability of Riboflavin and Lupeol after 30 ns and continued to stable until 100 ns (Fig. 8A). Riboflavin and Lupeol closely followed each other than Doxycycline. The control drug exhibited a minor fluctuation between 12 to 18 ns, stabilized until 85 ns, and then showed a slight upward movement, becoming stable again with a downward movement near 100 ns. The RMSF analysis showed fluctuations in a narrow range (Fig. 8B). The mean RMSF varied from 1.05 ± 0.78 to 1.40 ± 1.07 Å, where Doxycycline scored the lowest and Riboflavin scored the highest. Although the RMSF graph begins with residue index 1, this corresponds to the actual sequence of the protein. Specifically, the first residue in the graph (index 1) corresponds to Phe110 in the protein sequence, the second residue (index 2) corresponds to Val111, and so on. This consistent pattern ensures that the fluctuations observed in the RMSF graph can be directly mapped to the biologically relevant residue positions, despite the indexing convention used by the simulation software.

Table 4. ADMET properties evaluation of the lead candidates and Doxycycline.

Parameters	Molecule	Riboflavin	Lupeol	Doxycycline
Physicochemical properties	Formula	$C_{17}H_{20}N_4O_6$	$C_{30}H_{50}O$	$C_{22}H_{24}N_2O_8$
	Molecular weight (g/mol)	376.4	426.7	444.4
	H-bond acceptors	8	1	9
	H-bond donors	5	1	6
	Molar refractivity	96.99	135.14	110.91
	TPSA	161.56 $Å^2$	20.23 $Å^2$	181.62 $Å^2$
Lipophilicity	iLOGP	1.63	4.72	1.82
	XLOGP3	-1.46	9.87	0.54
	WLOGP	-1.68	8.02	-0.50
	MLOGP	-0.54	6.92	-2.08
	Silicos-IT Log P	1.09	6.82	-0.98
	Consensus Log P	-0.19	7.27	-0.24
Pharmacokinetics	GI absorption	Low	Low	Low
	CYP1A2	No	No	No
	CYP2C19	No	No	No
	CYP2C9	No	No	No
	Log Kp	-9.63 cm/s	-1.90 cm/s	-8.63 cm/s
Water solubility (ESOL)	Log S	-1.31	-8.64	-2.94
	Solubility (mg/ml)	1.85E+01	9.83E-07	5.07E-01
	Solubility (mol/l)	4.93E-02	2.30E-08	1.14E-03
	Class	Very soluble	Poorly soluble	Soluble
Drug likeness	Lipinski (violations)	0	1	1
	Bioavailability score	0.55	0.55	0.11
Medicinal chemistry	PAINS (alerts)	0	0	0
	Synthetic accessibility	3.84	5.49	5.25
Toxicity	Acute inhalation toxicity	No	No	No
	Acute oral toxicity	No	Yes	No
	Acute dermal toxicity	No	No	No
	Eye irritation and corrosion	Yes	No	Yes
	Skin sensitization	No	No	No
	Skin irritation and corrosion	No	Yes	No

Table 5. Molecular dynamics simulation trajectory analysis of the leads and Doxycycline.

Tested systems	PL RMSD (Å)	RMSF (Å)	Rg (Å)	SASA (Å^2)
Riboflavin	2.92 ± 0.41	1.40 ± 1.07	3.96 ± 0.09	183.01 ± 39.93
Lupeol	3.04 ± 0.55	1.23 ± 1.03	4.26 ± 0.03	235.24 ± 38.18
Doxycycline (control)	2.11 ± 0.43	1.05 ± 0.78	3.85 ± 0.04	260.95 ± 30.59

The radius of gyration (Rg) study further corroborated the drug candidacy of the two lead compounds, as both exhibited stability without any drastic fluctuations (Fig. 8C). Lupeol maintained a very steady trajectory, with fluctuations less than (0.2 Å). Riboflavin also maintained steady trajectory but at around 35 to 52 ns, it showed a minor downward movement, during which it intersected with Doxycycline. From 52 ns onwards, Riboflavin stabilized, maintaining a steady distance from both Doxycycline and Lupeol. Doxycycline demonstrated a few initial movements from 0 to 5 ns, but after 5 ns, it remained stable throughout the 100 ns. The SASA analysis bolstered the drug candidacy of the two leads as mean SASA score was lower for the two leads compared to Doxycycline (Table 5). The lowest mean SASA score was found in Riboflavin (183.01 ± 39.93) Å^2, followed by Lupeol (235.24 ± 38.18) Å^2, and Doxycycline (260.95 ± 30.59) Å^2. The trajectory graph elucidated the compactness of the two leads with the progression of time (Fig. 8D). Riboflavin and Lupeol showed minor primary movements from 0 to 55 ns, after which they maintained a consistent distance with each other and demonstrated a steady downward trend until 100 ns. Doxycycline also displayed a downward stabilization trend from around 50 ns until 88 ns, after which it showed a slight upward movement from 88 to 96 ns, and became stabilized again near 100 ns.

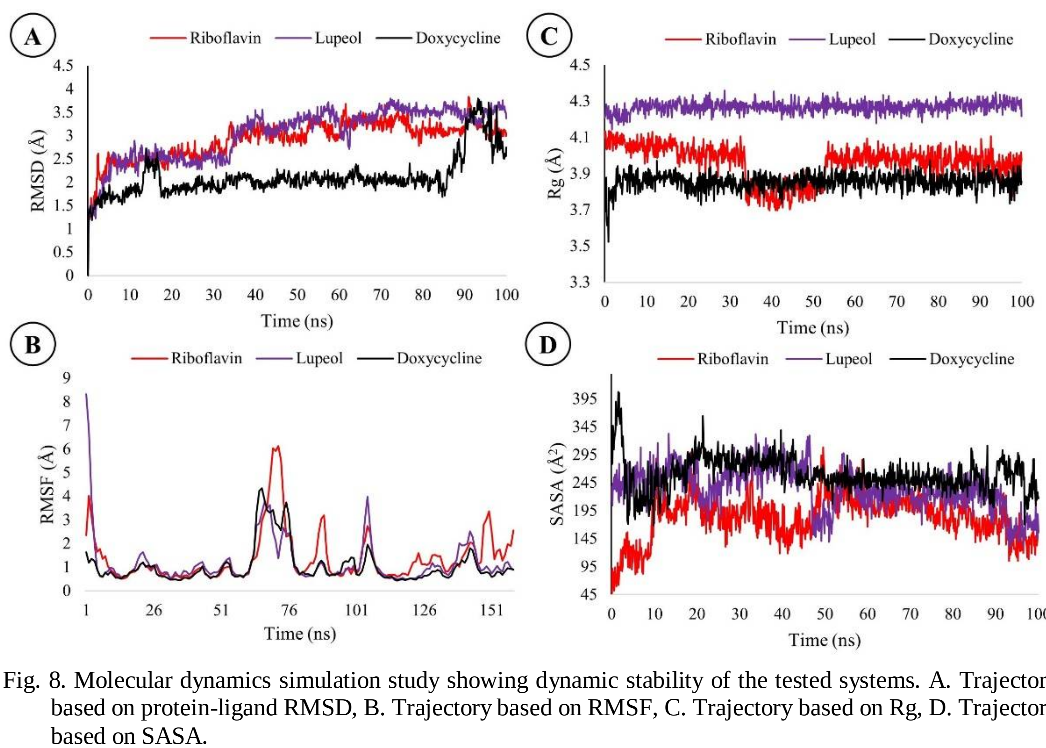

Fig. 8. Molecular dynamics simulation study showing dynamic stability of the tested systems. A. Trajectory based on protein-ligand RMSD, B. Trajectory based on RMSF, C. Trajectory based on Rg, D. Trajectory based on SASA.

The protein-ligand contact analysis revealed that Riboflavin formed the most extensive protein-ligand interactions, surpassing both Doxycycline and Lupeol (Fig. 9). Riboflavin exhibited the highest interaction fraction with Phe110, followed by His175, His190, and other residues (Fig. 9A), signifying its robust binding potential. Lupeol, which showed predominant hydrophobic interactions, formed its strongest contacts with Tyr393, followed by Asp185 and Leu188 (Fig. 9B), underscoring the role of nonpolar interactions in its binding affinity. Doxycycline demonstrated the highest interaction with Tyr420, followed by Asp185 and Leu187 (Fig. 9C), reflecting its distinct interaction pattern. These variations in binding profiles suggest differential stability and affinity of the compounds within the active site, emphasizing the importance of diverse interactions, especially hydrophobic and hydrogen bonding, in determining the efficacy of ligand binding.

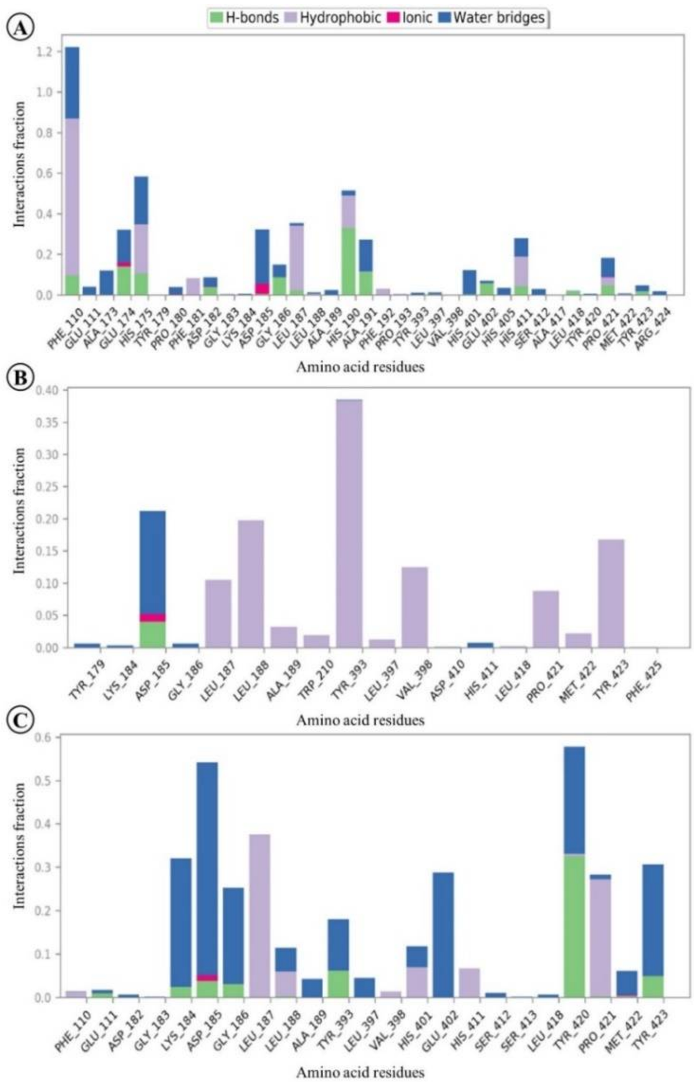

Fig. 9. Evaluation of protein-ligand contacts during molecular dynamics simulation. A. Riboflavin, B. Lupeol, C. Doxycycline.

PCA and Gibbs FEL

The PCA and Gibbs FEL analyses provided crucial insights into the essential dynamics and conformational stability of Riboflavin and Lupeol compared to Doxycycline (Fig. 10).

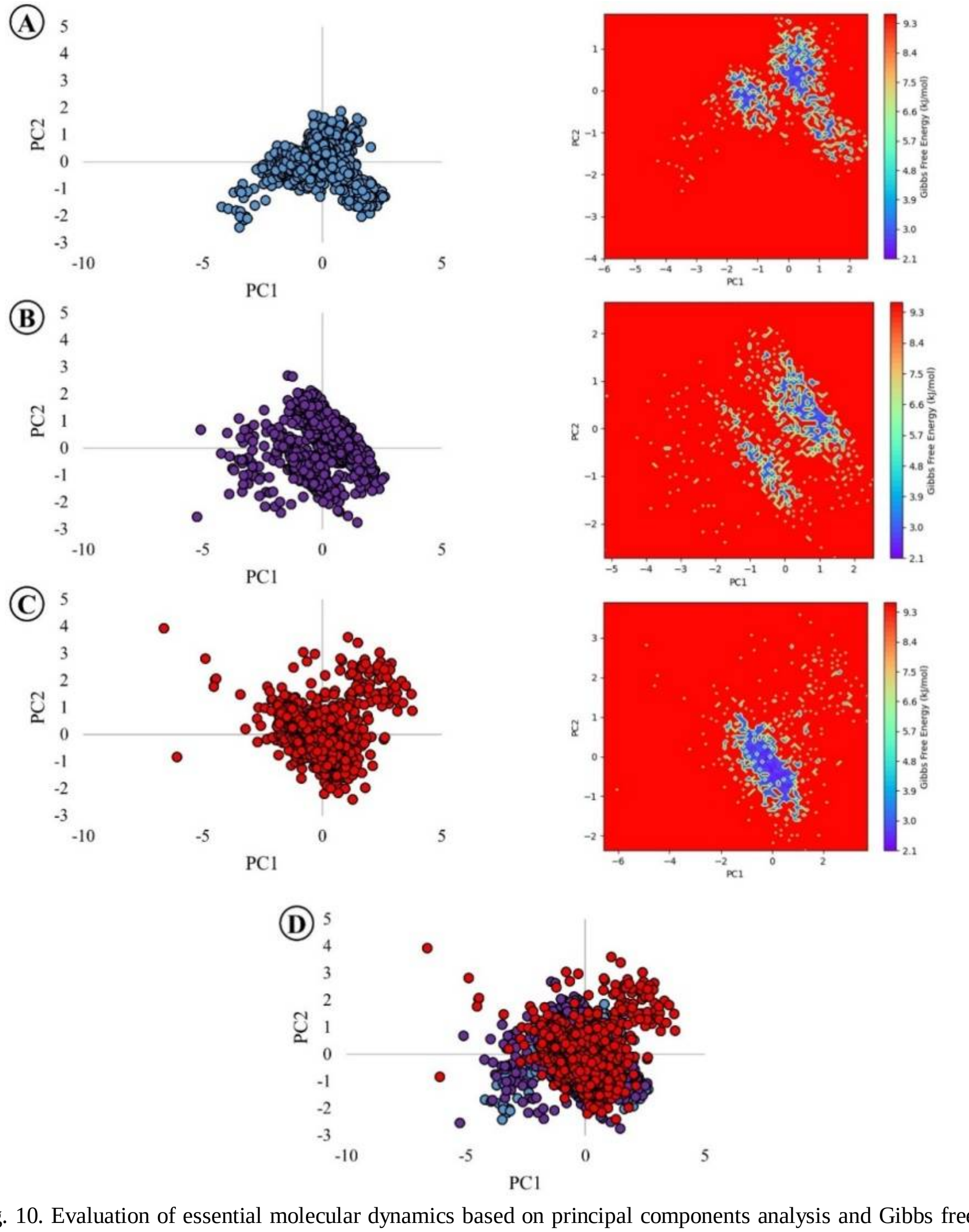

Fig. 10. Evaluation of essential molecular dynamics based on principal components analysis and Gibbs free energy landscapes. A. Riboflavin, B. Lupeol, C. Doxycycline, D. Superimposition of the two leads and Doxycycline.

The PCA phase-space distribution indicated that Riboflavin exhibited the highest degree of compactness, followed by Lupeol and Doxycycline, suggesting that Riboflavin maintains the most stable conformation during simulation. This was further corroborated by the Gibbs FEL analysis, which underscored the stability of Riboflavin by displaying a more centralized and extensive low-energy region (denoted by blue space), reflecting its preference for energetically favorable conformations (Fig. 10). Lupeol showed moderate stability, with a relatively smaller low-energy region, while Doxycycline displayed the least stable dynamics, with more dispersed energy states. These findings suggest that both Riboflavin and Lupeol demonstrate superior conformational stability compared to Doxycycline, potentially enhancing their suitability as drug candidates. The PCA and Gibbs FEL analyses align with previously published structure-based drug design study on *Chamaecostus cuspidatus* targeting DPP4 (Ahmed and Rahman, 2024).

Molecular reactivity evaluation

Molecular reactivity analysis revealed the energy levels of the electrons in the HOMO and LUMO states (Fig. 11). The energy of the HOMO state was the highest for Riboflavin (-6.496 eV), followed by Lupeol (-6.344 eV), and Doxycycline (-5.748 eV). For the LUMO state, the

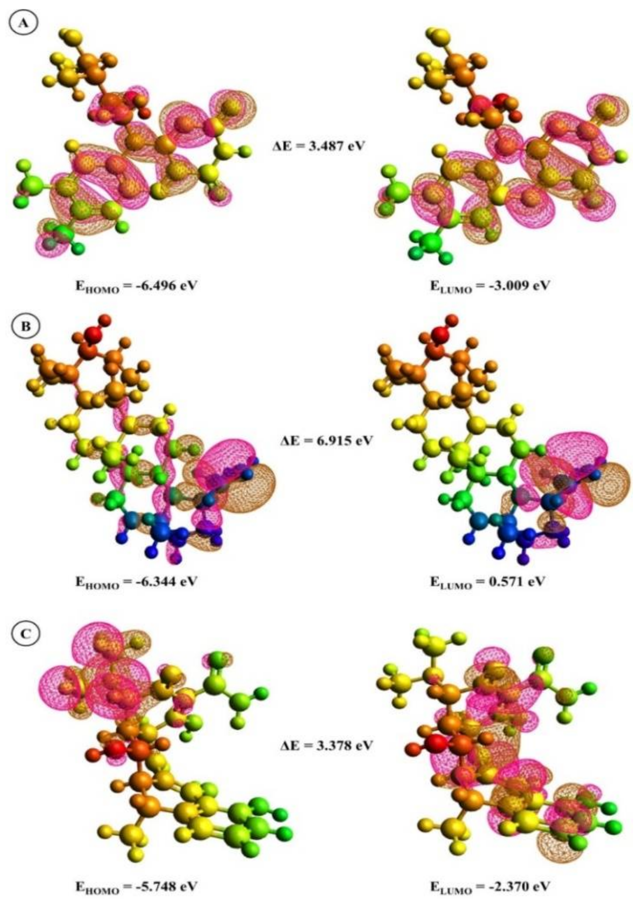

Fig. 11. DFT-based molecular reactivity analysis of the lead compounds and control drug. A. Riboflavin, B. Lupeol, C. Doxycycline (control).

highest energy was recorded for Riboflavin (-3.009 eV), followed by Doxycycline (-2.370 eV), and Lupeol (0.571 eV). The band energy gap (ΔE) was 3.487, 6.915, and 3.378 eV for Riboflavin, Lupeol, and Doxycycline, respectively (Fig. 11). The HOMO represents the orbital with the highest energy-containing electrons in a molecule. The electrons in the HOMO are generally the most reactive due to their high energy state and are thus the easiest to excite or donate to another molecule. The LUMO is the lowest energy orbital that does not contain electrons but can accept them. The LUMO is critical for understanding molecular interactions, as it is the orbital most likely to accept electrons (Paul *et al.,* 2023). The energy difference between HOMO and LUMO plays a critical role in understanding the molecular reactivity and kinetic stability of the lead compounds (Ahmed *et al*., 2023a). Doxycycline revealed the highest molecular reactivity with its lowest ΔE score of 3.378 eV. Riboflavin demonstrated closely similar results to Doxycyline with band energy gap of 3.487 eV. Lupeol showed the highest band energy gap of 6.915 eV and became the least reactive and most kinetically stable compound. The molecular reactivity results of the present investigation were congruent to the DFT analysis of *Amberboa ramosa* phytocompounds (Paul *et al.*, 2023).

With advanced computational biology techniques, our current investigation integrates classical plant taxonomy with drug design endeavor. This study would enrich the floristics knowledge of Liliopsida in Rajbari district and promote the discovery of anticancer agents targeting colorectal cancer. Furthermore, the study will encourage future floristics research to integrate taxonomic insights with bioinformatics, facilitating successful drug discovery from natural compounds and paving the way for exploring alternative medicines.

Acknowledgements

The first author extends her gratitude to the University Grant Commission of Bangladesh for granting the PhD Fellowship that facilitated this research. The authors thank Bangladesh National Herbarium for granting access to their herbarium materials. Additionally, the authors appreciate the information on the traditional uses of medicinal plant species shared by the local communities.

References

Ahmed, M.H., Karkush, S.I., Ali, S.A. and Mohammed, A.A. 2024. Phytochemicals: A new arsenal in drug discovery. Int. J. Med. Sci. Dent. Health. **10**(01): 29–44.

Ahmed, S.S. and Rahman, M.O. 2024. From Flora to Pharmaceuticals: 100 new additions to angiosperms of Gafargaon subdistrict in Bangladesh and unraveling antidiabetic drug candidates targeting DPP4 through *in silico* approach. PLoS One **19**(3): e0301348.

Ahmed, S.S., Suchana, L., Sultana, N. and Rahman, M.O. 2023a. Unveiling cervical cancer therapeutics from *Abrus precatorius* and *Aphanamixis polystachya*: Insights from molecular docking, dynamics simulation, MM/GBSA and DFT analyses. S. Afr. J. Bot. **163**: 561–579.

Ahmed, S.S., Al-Mamun, A., Hossain, S.I., Akter, F., Ahammad, I., Chowdhury, Z.M. and Salimullah, M. 2023b. Virtual screening reveals liquiritigenin as a broad-spectrum inhibitor of SARS-CoV-2 variants of concern: An *in silico* study. J. Biomol. Struct. Dyn. **41**(14): 6709–6727.

Ahmed, Z.U., Begum, Z.N.T. Hassan M.A., Khondker, M., Kabir, S.M.H., Ahmad, M., Ahmed, A.T.A., Rahman, A.K.A. and Haque, E.U. (Eds.) 2008. *Encyclopedia of Flora and Fauna of Bangladesh*, Vol. **12**. Asiatic Society of Bangladesh, Dhaka

Ara, H. and Hassan, M.A. Araceae. 2019. In: Ara, H. and Uddin, S.N. (Eds), Flora of Bangladesh. Fasc. 75. Bangladesh National Herbarium, Dhaka.

Arefin, M.K., Rahman, M.M., Uddin, M.Z. and Hassan, M.A. 2011. Angiosperm flora of Satchari National Park, Habiganj, Bangladesh. Bangladesh J. Plant Taxon. **18**(2): 117–140.

Bajad, N.G., Rayala, S., Gutti, G., Sharma, A., Singh, M., Kumar, A. and Singh, S.K. 2021. Systematic review on role of structure based drug design (SBDD) in the identification of anti-viral leads against SARS-Cov-2. Curr. Res. Pharmacol. Drug Discov. **2**: 100026.

BBS (Bangladesh Bureau of Statistics) 2022. Monthly Statistical Bulletin. Statistics Division, Ministry of Planning, Government of the People's Republic of Bangladesh.

Bendardaf, R., Buhmeida, A., Hilska, M., Laato, M., Syrjänen, S., Syrjänen, K., Collan, Y. and Pyrhönen, S. 2010. MMP-9 (gelatinase B) expression is associated with disease-free survival and disease-specific survival in colorectal cancer patients. Cancer Investig. **28**(1): 38–43.

Borba, J.V., Alves, V.M., Braga, R.C., Korn, D.R., Overdahl, K., Silva, A.C., Hall, S.U.S., Overdahl, E., Kleinstreuer, N., Strickland, J., Allen, D., Andrade, C.H., Muratov, E.N. and Tropsha, A. 2022. STopTox: An *in silico* alternative to animal testing for acute systemic and topical toxicity. Environ. Health Perspect. **130**(2): 027012.

Cronquist, A. 1981. An integrated system of classification of flowering plants. Columbia University Press, New York, pp. 1–1262.

Daina, A., Michielin, O. and Zoete, V. 2017. SwissADME: A free web tool to evaluate pharmacokinetics, drug-likeness and medicinal chemistry friendliness of small molecules. Sci. Rep. **7**(1): 42717.

Guex, N. and Peitsch, M.C. 1997. SWISS-MODEL and the Swiss-Pdb Viewer: An environment for comparative protein modeling. Electrophoresis **18**(15): 2714–2723.

Haque, A.K.M.K., Khan, S.A., Uddin, S.N. and Shetu, S.S. 2018. An annotated checklist of the Angiospermic flora of Rajkandi Reserve Forest of Moulvibazar, Bangladesh. Bangladesh J. Plant Taxon. **25**(2): 187–207.

Heywood, V. 2004. Modern approaches to floristics and their impact on the region of SW Asia. *Turk. J. Bot.* **28**: 7–16.

Hooker, J.D. 1872-1897. The Flora of British India, Vols. **1**–**7**. L. Reeve & Co., Ashford, Kent, UK.

Hossain, G.M., Khan, S.A., Rahim, M.A., Rahman, M.S. and Islam, K.M.N. 2021. Floristic composition of the coastal district Satkhira, Bangladesh. Bangladesh J. Plant Taxon. **28**(1): 97–124.

Hossain, G.M, Khan, S.A., Shetu, S.S., Rahman, M.S., Ahmed, F.A. and Ali, M.H. 2022. Floristic survey of vascular plants in coastal district Bagerhat of Bangladesh. Bangladesh J. Plant Taxon. **29**(1): 43–78.

Huq, A.M. 2019. Plant Names of Bangladesh. Ashrafia Boi Char, Banglabazar, Dhaka, 599 pp.

Islam, M.R., Uddin, M.Z. and Hassan, M.A. 2009. An assessment of the angiospermic flora of Ramgarh upazila of Khagrachhari district, Bangladesh. Bangladesh J. Plant Taxon. **16**(2): 115–140.

Islam, M.S. and Khan, S.A. 2024. A preliminary study of the pteridophytes, gymnosperms and monocotyledons in the Chapainawabganj district's flora of Bangladesh. Bangladesh J. Plant Taxon. **31**(1): 83–99.

Islam, M.R., Hossain, G.M. and Rahman, M.M. 2022. An annotated checklist of the vascular flora of coastal mangrove ecosystems of Barguna district, Bangladesh. Bangladesh J. Plant Taxon. **29**(2): 403–429.

Islam, S.I., Ahmed, S.S., Habib, N., Ferdous, M.A., Sanjida, S. and Mou, M.J. 2023. High-throughput virtual screening of marine algae metabolites as high-affinity inhibitors of ISKNV major capsid protein: An analysis of in-silico models and DFT calculation to find novel drug molecules for fighting infectious spleen and kidney necrosis virus (ISKNV). Heliyon **9**(6): e16383.

Khan, M.S. and Alam, M.K. 1977. Commelinacae. In: Khan, M.S. (Ed.), Flora of Bangladesh. Fasc. 4. Bangladesh National Herbarium, Dhaka.

Khan, M.S. and Halim, M. 1985. Hydrocharitaceae. In: Khan, M.S. (Ed.), Flora of Bangladesh. Fasc. 28. Bangladesh National Herbarium, Dhaka

Khan, S.A., Hossain, G.M., Shetu, S.S., Rahim, M.A., Islam, M.S., Ahmed, F.A. and Fairy, R.H. 2021. A preliminary taxonomic study on the flora of Rangpur district, Bangladesh. Bangladesh J. Plant Taxon. **28**(2): 329–365.

Khanam, R. and Khan, S.A. 2020. Angiosperms in Narsingdi district of Bangladesh: Class Liliopsida. Bangladesh J. Plant Taxon. **27**(2): 391–405.

Khanam, R., Khan, S.A. and Rahim, A. 2020. Angiosperms in Narsingdi district of Bangladesh: Class Magnoliopsida. Bangladesh J. Plant Taxon. **27**(1): 153–171.

Kim, H.S., Luo, L., Pflugfelder, S.C. and Li, D.Q. 2005. Doxycycline inhibits TGF-β1–induced MMP-9 via SMAD and MAPK pathways in human corneal epithelial cells. Invest. Opthalmol. Vis. Sci. **46**(3): 840–848.

Mahmudah, Z., Islam, M.M, Haque, T. and Uddin, M.Z. 2017. Taxonomic enumeration of angiosperm flora of Sreenagar upazila, Munshiganj, dhaka, Bangladesh. J. Asiat. Soc. Bangladesh, Sci. **43**(2): 161–172.

Minibaeva, G., Ivanova, A. and Polishchuk, P. 2023. EasyDock: Customizable and scalable docking tool. J. Cheminform. **15**(1): 102.

O'Boyle, N.M., Morley, C. and Hutchison, G.R. 2008. Pybel: A Python wrapper for the OpenBabel cheminformatics toolkit. Chem. Cent. J. **2**: 1–7.

Paul, R.K., Ahmad, I., Patel, H., Kumar, V. and Raza, K. 2023. Phytochemicals from *Amberboa ramosa* as potential DPP-IV inhibitors for the management of Type-II diabetes mellitus: Inferences from in-silico investigations. J. Mol. Struct. **1271**: 134045.

POWO 2024. Plants of the World Online. www.plantsoftheworldonline.org. Facilitated by the Royal Botanic Gardens, Kew

Prain, D. 1903. Bengal Plants, Vols. **1** and **2**. Reprint 1963. Botanical Survey of India, Calcutta.

Rahman M.O and Alam, M.T. 2013. A taxonomic study on the angiosperm flora of Trishal upazila, Mymensingh. Dhaka Univ. J. Biol. Sci. **22**(1): 63–74.

Rahman, M.O. and Hassan, M.A. 1995. Angiospermic flora of Bhawal National Park, Gazipur (Bangladesh). Bangladesh J. Plant Taxon. **2**(1&2): 47–80.

Rahman, M.O., Antara, R.T., Begum, M. and Hassan, M.A. 2012. Floristic diversity of Dhamrai upazila of Dhaka with emphasis on medicinal plants. Bangladesh J. Bot. **41**(1): 71–85.

Rahman, M.O., Begum, M. and Ullah, M.W. 2013. Angiosperm Flora of Sadar Upazila of Munshiganj District, Bangladesh. Bangladesh J. Plant Taxon. **20**(2): 213–231.

Rahman M.O., Hassan, S. and Begum, M. 2019a. Floristic study in Lalpur upazila of Natore district, Bangladesh: Identification, distribution and economic potential. J. Asiat. Soc. Bangladesh (Science) **45**(1): 71–91.

Rahman, M.O., Sayma, N.J. and Begum, M. 2019b. Angiospermic flora of Gafargaon upazila of Mymensingh district focusing on medicinally important species. Bangladesh J. Plant Taxon. **26**(2): 269–283.

Rahman, M.O., Ahmed, S.S., Alqahtani, A.S., Cakilcioğlu, U. and Akbar, M.A. 2024. Insight into novel inhibitors from *Sterculia urens* against Cholera via pharmacoinformatics and molecular dynamics simulation approaches. J. Biomol. Struct. Dyn. **42**(19): 10022–10043.

Rahman, M.S., Hossain, M.G., Khan, S.A. and Uddin, S.N. 2015. An annotated checklist of the vascular plants of Sundarban mangrove forest of Bangladesh. Bangladesh J. Plant Taxon. **22**(1): 17–41.

Rashid, Z.A. and Bardaweel, S.K. 2023. Novel matrix metalloproteinase-9 (MMP-9) inhibitors in cancer treatment. Int. J. Mol. Sci. **24**(15): 12133.

Rizvi, S.M.D., Shakil, S. and Haneef, M. 2013. A simple click by click protocol to perform docking: AutoDock 4.2 made easy for non-bioinformaticians. EXCLI J. **12**: 831–857.

Rowsell, S., Hawtin, P., Minshull, C.A., Jepson, H., Brockbank, S.M., Barratt, D.G., Slater, A.M., McPheat, W.L., Waterson, D., Henney, A.M. and Pauptit, R.A. 2002. Crystal structure of human MMP9 in complex with a reverse hydroxamate inhibitor. J. Mol. Biol. **319**(1): 173–181.

Said, A.H., Raufman, J.P. and Xie, G. 2014. The role of matrix metalloproteinases in colorectal cancer. Cancers **6**(1): 366–375.

Sajib, N.H., Uddin, S.B. and Islam, M.M. 2014. Angiospermic plant diversity of Subarnachar upazila in Noakhali, Bangladesh. J. Asiat. Soc. Bangladesh, Sci. **40**(1):39–60.

Sarkar, K., Debbarma, M., Debnath, S., Ghosh, R. and Sil, S.K. 2024. In silico identification of dual HDAC8 and MMP9 inhibitors by pharmacophore modeling, molecular docking, and molecular dynamics simulation studies for development of antitumour agent. Interactions **245**(1): 1–24.

Sarker, K., Islam, M.R., Uddin, M.Z., and Hassan, M.A. 2013. Angiosperm flora of Manikgonj sadar upazila, Bangladesh. J. Asiat. Soc. Bangladesh, Sci. **39**(2): 147–166.

Shrivastava, A.K., Keshari, M., Neupane, M., Chaudhary, S., Dhakal, P.K., Shrestha, L., Palikhey, A., Yadav, C.K., Lamichhane, G., Shekh, M.U. and Yadav, R.K. 2023. Evaluation of antioxidant and anti-inflammatory activities, and metabolite profiling of selected medicinal plants of Nepal. J. Trop. Med. **2023**(1): 6641018.

Siddiqui, K.U., Islam, M.A., Ahmed, Z.U., Begum, Z.N.T., Hassan, M.A., Khondker, M., Rahman, M.M., Kabir, S.M.H., Ahmed, A.T.A., Rahman, A.K.A. and Haque, E.U. (Eds). 2007. Encyclopedia of Flora and Fauna of Bangladesh, Vol. **11**. Asiatic Society of Bangladesh, Dhaka, Bangladesh.

Singh, H.B. and Subramaniam, B. 2008. Field Manual on Herbarium Techniques. National Institute of Science Communication and Information Resources, pp. 1–297.

Snyder, H.D. and Kucukkal, T.G. 2021. Computational chemistry activities with Avogadro and ORCA. J. Chem. Educ. **98**(4): 1335–1341.

Sultana, M. 2012. Taxonomic and ethnobatanical studies on the angiospermic flora of Patuakhali district In Bangladesh. Ph.D. Thesis (Unpublished). Department of Botany, University of Dhaka.

Tabassum, R. 2015. Angiospermic flora of Gazipur district, Bangladesh. Doctoral Dissertation. Department of Botany, University of Dhaka, pp. 1–707.

Tian, W., Chen, C., Lei, X., Zhao, J. and Liang, J. 2018. CASTp 3.0: Computed atlas of surface topography of proteins. Nucleic Acids Res. **46**(W1): W363–W367.

Uddin, M.Z. and Hassan, M.A. 2010. Angiosperm diversity of Lawachara National Park (Bangladesh): A preliminary assessment. Bangladesh J. Plant Taxon. **17**(1): 9–22.

Vivek-Ananth, R.P., Mohanraj, K., Sahoo, A.K. and Samal, A. 2023. IMPPAT 2.0: An enhanced and expanded phytochemical atlas of Indian medicinal plants. ACS Omega **8**(9): 8827–8845.

(Manuscript received on 3 January 2024; revised on 23 November 2024)